Astron. Astrophys. 333, 163–171 (1998)

ASTRONOMY AND ASTROPHYSICS

Hubble Space Telescope ultraviolet spectroscopy of the supersoft X-ray binaries CAL 83 and RX J0513.9−6951⋆

B.T. Gänsicke[1], **A. van Teeseling**[1], **K. Beuermann**[1], **and D. de Martino**[2]

[1] Universitäts-Sternwarte, Geismarlandstrasse 11, D-37083 Göttingen, Germany
[2] Osservatorio Astronomico di Capodimonte, Via Moiariello 16, I-80131 Naples, Italy

Received 13 June 1997 / Accepted 23 January 1998

Abstract. We present Hubble Space Telescope ultraviolet observations with the Goddard High Resolution Spectrograph of the supersoft X-ray binaries CAL 83 and RX J0513.9−6951 in the Large Magellanic Cloud. Both sources show a remarkably similar spectrum with an almost flat continuum and weak N v and O v emission lines. The neutral hydrogen column densities derived from the broad Lyα profile are $N_{\rm HI} = (6.5 \pm 1.0) \times 10^{20}$ cm^{-2} for CAL 83 and $N_{\rm HI} = (5.5 \pm 1.0) \times 10^{20}$ cm^{-2} for RX J0513.9−6951. These column densities are very similar to the galactic foreground column density, indicating that the two sources are located on the near side of the LMC. With this independent estimate of $N_{\rm HI}$, we find that the X-ray source in CAL 83 has a luminosity of $(0.7 - 2) \times 10^{37}$ ergs s^{-1}. The inferred radius for the supersoft source in CAL 83 is consistent with the radius of a white dwarf which has not significantly expanded due to the shell burning. For RX J0513.9−6951, we find a luminosity of $(2.5 - 9) \times 10^{37}$ ergs s^{-1}. The long-term ultraviolet light curve of CAL 83 shows a rare bright state during which the ultraviolet flux has doubled.

Key words: accretion, accretion disks – binaries: close – stars: atmospheres – stars, individual: CAL 83, RX J0513.9–6951 – ultraviolet: stars

1. Introduction

CAL 83 is the prototype of a small class of interacting close binaries which have luminosities comparable to those of low-mass X-ray binaries, but which display a very soft X-ray spectrum with almost all flux below 0.5 keV. Several objects with similar X-ray properties have been discovered with ROSAT, *observationally* defining the class of supersoft X-ray sources. Greiner (1996) presents a collection of recent papers on these sources. So far only a dozen of supersoft X-ray sources have been identified as close binaries like CAL 83. In the broadly accepted model for these supersoft X-ray binaries (SSXBs), a white dwarf accretes matter at a rate sufficient for stable hydrogen shell burning, either quasi-steady or after a mild helium shell flash (van den Heuvel et al. 1992; Sion & Starrfield 1994). Hitherto, the luminosities of SSXBs have been subject to some debate (e.g. van Teeseling et al. 1996). Fits to the observed X-ray spectra provide evidence for the white dwarf nature of the accreting object and suggest luminosities of $10^{36} - 10^{38}$ergs s^{-1}, close to the Eddington luminosity of a white dwarf. The exact value of the luminosity, however, is difficult to determine due to the largely unknown soft X-ray absorption.

Additional observational evidence for the white dwarf nature of the accreting object has recently been inferred for RX J0513.9−6951, henceforth RX J0513. At optical wavelengths, this ROSAT-discovered SSXB (Schaeidt et al. 1993) displays weak emission lines nearby Hα, Hβ, and He II λ 4686, which have been interpreted as evidence for a bipolar jet (Crampton et al. 1996). Identifying the observed jet velocity of ~ 4000 km s^{-1} with the escape velocity of the compact object, Southwell et al. (1996) argued that the accreting star is likely to be a white dwarf.

Interest for RX J0513 has been stimulated by its peculiar variability. While the source occasionally turns on in the ROSAT band (Schaeidt et al. 1993; Schaeidt 1996), recent optical investigations show that these X-ray on states are accompanied by *optical low states* (Reinsch et al. 1996). These optical low states have a recurrence time of several months (Southwell et al. 1996). In the hydrogen-burning white dwarf model, this reversed variability at X-ray and optical wavelengths can be explained by a changing radius of the white dwarf photosphere, perhaps due to small fluctuations in the accretion rate onto the hydrogen-burning white dwarf, and the subsequent change in the amount of irradiation of the accretion disk: during the X-ray turn-on and optical decline, the white dwarf photosphere contracts considerably at almost constant luminosity, accompanied with an increase of the effective temperature. The X-ray on states (and optical low states) occur when the white dwarf photosphere becomes sufficiently hot to radiate in the ROSAT band-pass (Pakull et al. 1993; Reinsch et al. 1996).

Hitherto, only IUE observations with modest spectral resolution have been obtained for CAL 83 and RX J0513, revealing

Send offprint requests to: B. Gänsicke (boris@uni-sw.gwdg.de)

⋆ Based on observations made with the NASA/ESA Hubble Space Telescope, obtained at the Space Telescope Science Institute, which is operated by the Association of Universities for Research in Astronomy, Inc., under NASA contract NAS 5-26555 and on observations made with the International Ultraviolet Explorer, retrieved from the IUE Final Archive

Table 1. HST GHRS/G140L observations of CAL 83 & RX J0513, covering the wavelength range 1150−1435Å

Dataset	Exposure start (UT)	Exposure time [sec]
CAL 83		
Z3HS0105T	10 Nov 1996 00:37:24	2774
RX J0513		
Z3HS0205T	13 Nov 1996 04:12:48	2774

Table 2. IUE observations of CAL 83 and RX J0513.

Image No.	Exposure start (UT)	Exposure time [sec]	Quality
CAL 83			
LWP04890L	Nov 25 1984	1320	$-^{1)}$
LWP12257L	Dec 11 1987	16080	+
LWP13902L	Aug 23 1988	12900	+
SWP24554L	Nov 24 1984	15060	+
SWP24560L	Nov 25 1984	1800	$-^{1)}$
SWP24563L	Nov 26 1984	5400	$-^{1)}$
SWP25309L	Feb 24 1985	21600	$+^{2)}$
SWP28390L	May 28 1986	30000	+
SWP30024L	Jan 05 1987	16320	+
SWP32511L	Dec 12 1987	14400	+
SWP33936L	Jul 17 1988	16860	+
SWP39995L	Oct 29 1990	24420	+
SWP40017L	Nov 01 1990	22800	+
SWP40047L	Nov 04 1990	22500	$+^{2)}$
SWP40075L	Nov 07 1990	22800	+
SWP40563L	Jan 11 1991	5700	$o^{3)}$
SWP40590L	Jan 14 1991	15480	+
RX J0513			
LWP22883L	Apr 25 1992	23100	+
LWP30953L	Jun 29 1995	19800	$-^{4)}$
SWP44467L	Apr 24 1992	24000	+
SWP50208L	Mar 14 1994	4500	$-^{1)}$
SWP55170L	Jun 29 1995	22800	+

Listed are the IUE frame number, the observation date, the exposure time and the quality of the data.

+ good data
o data to be used with care
− data useless
1) Underexposed
2) Strongly affected by cosmic hits
3) Low S/N exposures
4) serendipitous image, no spectrum

a blue continuum overlayed with emission lines of N v and He ii and with weak absorption lines (Crampton et al. 1987; Pakull et al. 1993). In this paper we present the first high-resolution ultraviolet spectra of CAL 83 and RX J0513, which allow us to address the origin of both absorption and emission lines. These observations are complemented with low resolution IUE archival spectra taken at different epochs, allowing the detection of a long-term variability at ultraviolet wavelengths.

2. HST/GHRS observations

Hubble Space Telescope (HST) observations of CAL 83 and RX J0513 were carried out on 1996 November 10 and 13, respectively (Table 1). At the time of the observations, the two stars were located in the continuous viewing zone of HST, so that one spacecraft orbit per source was sufficient to obtain a well-exposed spectrum. Due to the faintness of the objects, the target acquisition was done with the Faint Object Spectrograph (FOS) with a subsequent switch to Side 1 of the Goddard High Resolution Spectrograph (GHRS). This procedure has been described in detail by Leitherer et al. (1994). The spectroscopic observations were performed in the ACCUM mode, using the G140L grating and the 2" Large Science Aperture (LSA). The central wavelength was set to 1292 Å yielding a spectral coverage of 1150−1435 Å with a nominal FWHM resolution of ~ 0.6 Å, corresponding to 125−150 $\mathrm{km\,s^{-1}}$. The spectra were processed through the standard data reduction pipeline at STScI, providing flux and wavelength calibrated spectra. The accuracy of these standard calibrations is limited as follows:

(a) Regular monitoring with the GHRS/G140L grating has revealed a continuous decrease of the sensitivity below 1200 Å. In August 1996, the response was reduced by 15% (5%) at 1150 Å (1200 Å) compared to the sensitivity just after the first Service Mission. We computed a correction function for this decreased sensitivity from G140L observations of the ultraviolet standard BD+28°4211, obtained only ten days after our observations of CAL 83 and RX J0513.

(b) An additional generic uncertainty of the flux at short wavelengths ($\lesssim 1180$ Å) exists: the *absolute* flux calibration of HST spectroscopy is based on the comparison between observations and model spectra of the white dwarf G191–B2B. However, G191–B2B has never been observed with the GHRS/G140L grating. The flux calibration of this setup is based on the comparison of GHRS/G140L and FOS/G130H spectra of BD+28°4211, where the FOS/G130H setup has been absolutely calibrated with the flux standard G191–B2B. As the FOS/G130H spectrum ends at ~ 1140 Å, the GHRS/G140L flux calibration remains necessarily uncertain at the shortest wavelengths.

(c) The FOS assisted target acquisition results in an ~ 0.35" uncertainty of the object position in the LSA of the GHRS. With the G140L grating, this translates into an uncertainty of about 200 $\mathrm{km\,s^{-1}}$ of the zero point of the wavelength calibration.

The GHRS spectra of CAL 83 and RX J0513, corrected for the decreased sensitivity, are shown in Fig. 1. Apart from the difference in total flux, the two objects look strikingly similar, containing a broad Lyα absorption profile as well as numerous strong absorption lines superposed on an almost flat continuum. The N v $\lambda\lambda$ 1239,43 resonance doublet is observed in both sources while significant emission of O v λ 1371 is present only

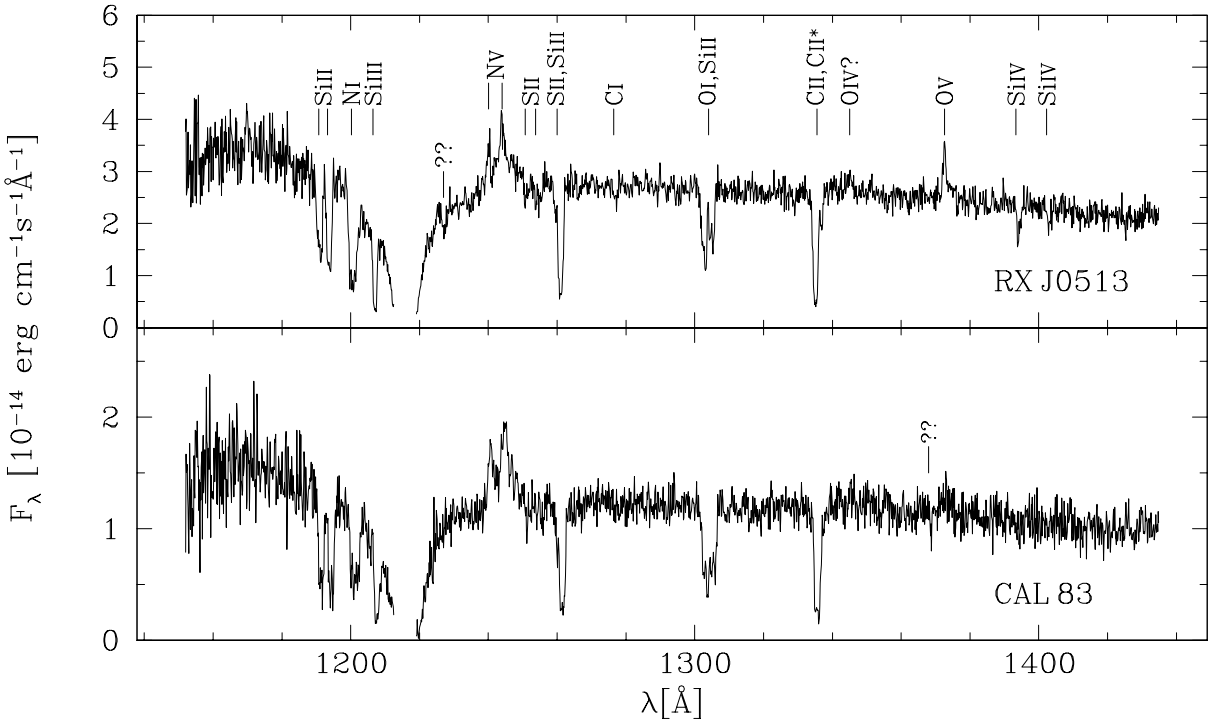

Fig. 1. HST spectrum of CAL 83 (bottom) and RX J0513 (top). The geocoronal emission line has been truncated.

in the spectrum of RX J0513. The signal-to-noise ratio (S/N) of the spectrum of CAL 83 (RX J0513) is ~ 5 (8) above Lyα but decreases to 2 (4) at 1150 Å. The slight decrease in flux below 1170 Å is very likely not real and due to the uncertain calibration described above.

3. Results

3.1. Comparison with IUE observations

Both CAL 83 and RX J0513 are known to be variable at optical and X-ray wavelengths on timescales much longer than the binary period (e.g. Pakull et al. 1993; Reinsch et al. 1996; Kahabka 1997; Alcock et al. 1997). In order to compare the flux level of our HST data with those of previous observations, we have retrieved all IUE spectra of both sources available from the archive (Table 2). All IUE observations were performed in the low-resolution mode (FWHM ~ 6 Å) through the large aperture. The spectra have been reprocessed with the IUE Final Archive procedures (NEWSIPS), yielding for low exposure levels a higher S/N than achieved in the original processing. The faintness of the objects required very long IUE exposures, resulting in a strong contamination of the spectra by cosmic hits. We have inspected all spectra for spurious features, which have been removed if possible. A flag for the quality of the individual spectra is given in Table 2.

For CAL 83, the number of IUE observations is sufficiently large to compile a long-term light curve which is shown in Fig. 2. During all IUE observations, CAL 83 was at the same flux level, except in one case during which the ultraviolet flux had increased by more than a factor of two. During the ultraviolet bright state, the spectrum was steeper than during the normal state, indicating a hotter source (Crampton et al. 1987). Bianchi & Pakull (1988) report that, at the time of the ultraviolet bright state, CAL 83 was also much brighter at optical wavelengths. For RX J0513, only two good SWP spectra are available: SWP44467L shows the source with a steeper spectrum and at a flux level ~ 2 lower than SWP55170L (see Fig. 5 of Gänsicke et al. 1996). The flux of our GHRS spectrum agrees well with that of SWP44467L. At optical wavelengths, RX J0513 is usually in a bright state (Southwell et al. 1996, see also Sect. 4.2); the HST and IUE observations suggest that this is also the case in the ultraviolet. It appears, therefore, that we have observed both sources in their normal states.

Table 3. Galactic coordinates, total and galactic neutral hydrogen column densities for CAL 83 and RX J0513 and for three comparison stars in the LMC

System	b	l	total $N_{\rm HI}$ [10^{20}cm^{-2}]	galactic $N_{\rm HI}$ [10^{20}cm^{-2}]
CAL 83	278.6	−31.3	$6.5 \pm 1.0^{(1)}$	$6.5^{(3)}$
RX J0513	280.8	−33.7	$5.5 \pm 1.0^{(1)}$	$8.4^{(3)}$
HD 36402	277.8	−33.0	-	$5.3^{(2)}, 6.2^{(3)}$
HD 38282	279.4	−31.7	-	$5.5^{(2)}, 5.8^{(3)}$
HD 269357	279.9	−33.4	-	$6.2^{(3)}$

$^{(1)}$This work $^{(2)}$Savage & de Boer (1981) $^{(3)}$Dickey & Lockman (1990), as implemented in EXSAS (Zimmermann et al. 1994)

3.2. Hydrogen column density and interstellar reddening

The observed broad Lyα absorption profile may be composed of different contributions. Absorption by interstellar neutral hydrogen along the line of sight is probably the dominant factor for CAL 83 and RX J0513. Fitting the observed Lyα absorption with a pure damping profile (e.g. Bohlin 1975) yields neutral hydrogen column densities of $N_{\rm HI} = (6.5 \pm 1.0) \times 10^{20}$ cm^{-2} for CAL 83 and $N_{\rm HI} = (5.5 \pm 1.0) \times 10^{20}$ cm^{-2} for RX J0513. However, because the intrinsic source spectrum could contain a rotationally and pressure broadened Lyα absorption line formed e.g. in the accretion disc, the derived $N_{\rm HI}$ is actually an *upper limit* to the total neutral hydrogen column density along the line of sight, which includes galactic and LMC interstellar absorption, as well as any possible intrinsic absorption within the binary system. Assuming the normal galactic gas-to-dust ratio (Bohlin et al. 1978), the Lyα column densities translate into a reddening of $E(B-V) \approx 0.13$. The available IUE LWP spectra are too noisy to put further constraints on the reddening using the 2200 Å feature.

The derived $N_{\rm HI}$ values are comparable to the values of the galactic foreground column density towards the LMC based on H I 21-cm observations, which vary between $\sim 3 \times 10^{20}$ cm^{-2} and $\sim 8 \times 10^{20}$ cm^{-2} (e.g. Fitzpatrick 1986; Bessell 1991). We compare in Table 3 the *total* neutral hydrogen column densities of CAL 83 and RX J0513 as derived from the HST spectra with the *galactic* foreground column densities computed with EXSAS (Zimmermann et al. 1994, based on the data of Dickey & Lockman 1990) for the corresponding lines of sight. These latter values have to be judged somewhat carefully, as the spatial resolution of the $N_{\rm H}$ survey by Dickey & Lockman (1990) is rather poor ($1^\circ \times 1^\circ$). The total neutral hydrogen column densities along the lines of sight towards CAL 83 and RX J0513 *within* the LMC have been estimated from the data of Rohlfs et al. (1984) to be $\sim 15 \times 10^{20}$ cm^{-2} and $\sim 6 \times 10^{20}$ cm^{-2}, respectively. We conclude that both sources are located on the near side of the LMC and that there is no evidence for a substantial intrinsic *neutral* hydrogen column density in CAL 83 or RX J0513 (see however Sect. 4.1).

In addition, Table 3 lists three bright LMC stars which have galactic neutral hydrogen column densities comparable to those obtained for CAL 83 and RX J0513. These three stars have a well-studied interstellar absorption line spectrum which will be used in Sect. 3.3 to discuss the origin of absorption features observed in CAL 83 and RX J0513.

3.3. Absorption lines

Our HST/GHRS spectra confirm the absorption lines at 1260 Å, 1300 Å, and 1335 Å detected in the IUE spectra of CAL 83 (Crampton et al. 1987; Bianchi & Pakull 1988) and RX J0513 (Pakull et al. 1993), and in the HST/FOS spectra of CAL 87 (Hutchings et al. 1995). Additional strong absorption lines at 1191 Å, 1194 Å, 1200 Å, and 1206 Å are present in the previously unobserved wavelength range below Lyα. The spectrum of RX J0513 also contains weak absorption lines at 1394 Å and 1404 Å. Table 4 summarizes the identifications and the measured equivalent widths for all absorption lines. Two absorption features, one at 1367.7 Å in the spectrum of CAL 83 and one at 1227.2 Å in the spectrum of RX J0513 could not be identified. We note that if the feature at 1227.2 Å is redshifted Lyα absorption in a high-velocity outflow (see Sect. 3.4), it would correspond to a velocity of $\sim +2800\,{\rm km\,s^{-1}}$. The formation of an *absorption* line in a redshifted outflow is, however, not straightforward to understand, and would suggest e.g. that the outflow is partly optically thick in Lyα or that the high-velocity matter is actually *inflow*. At wavelengths shorter than Lyα, the S/N is much lower, which may prevent the detection of an absorption feature near $-2800\,{\rm km\,s^{-1}}$.

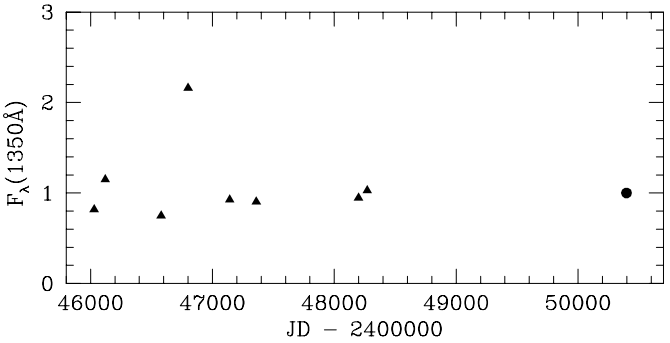

Fig. 2. Ultraviolet long-term variability of CAL 83 from IUE ▲ and HST ● observations. Plotted is the 1300−1400 Å average flux F_λ in $10^{-14}\,{\rm ergs\,cm^{-2}s^{-1}\AA^{-1}}$.

All identified lines coincide with interstellar absorption features, and have equivalent widths which are compatible with the LMC membership of the two SSXBs. As the HST/GHRS spectra of CAL 83 and RX J0513 are the first high-resolution ultraviolet spectra of SSXBs obtained so far, we discuss the likely interstellar origin of the absorption lines in more detail below.

Interstellar absorption in the direction of the LMC consists of several components: (a) Weak absorption lines from low-ionization species are formed in the local interstellar medium close to zero velocity. (b) Interstellar matter at high galactic latitudes ($|z| > 1$ kpc) yields strong absorption lines extending to large positive velocities ($\sim 120\,{\rm km\,s^{-1}}$). In the galactic halo, hot gas causes absorption by highly ionized species as Si IV or C IV (Savage & de Boer 1979). (c) Interstellar lines originating in the LMC have velocities of $v \gtrsim 190\,{\rm km\,s^{-1}}$. The LMC is probably also surrounded by hot gas (de Boer & Savage 1980), yielding a high-velocity component in the lines of Si IV or C IV. The high level of complexity in the interstellar absorption spectrum towards the LMC, including several absorption features at intermediate velocities, is depicted in an ultraviolet spectral atlas of supernova 1987A (Blades et al. 1988).

In Table 4, we compare the interstellar equivalent widths measured for CAL 83 and RX J0513 from our HST spectra with values compiled from the literature for the three LMC stars listed in Table 3. These three stars were chosen from the small sample of LMC objects which have a well-studied interstellar absorption spectrum in order to show typical variations of the

Table 4. Identification and equivalent width measurements of the absorption lines in CAL 83 & RX J0513. The values for three comparison stars are compiled from Savage & de Boer (1979, 1981), de Boer & Savage (1980) and de Boer et al. (1980). All equivalent widths (EW) are given in [mÅ].

Ion	$\lambda_{\rm lab}$ [Å]	CAL 83	RX J0513	HD36402	HD38282	HD269357
Si II	1190.70	1200 ± 100	1000 ± 100			
Si II	1193.29	1250 ± 100	1000 ± 100	$750^{g)}$	$490^{g)}$	$740^{g)}$
N I	1199.55, 1200.22, 1200.71	$1600 \pm 150^{a)}$	$1800 \pm 150^{a)}$	$210:{}^{g,n)}$	$250:{}^{g,n)}$	$400:{}^{g,m)}$
Si III	1206.51	1400 ± 100	1080 ± 100	$790^{g)} + 610^{l)}$	$390^{g)}$	$820^{g)}$
S II	1259.52	$1900 \pm 150^{b)}$	$1520 \pm 150^{b)}$	$120^{g)}$	$170^{g)} + 700:{}^{l)}$	$170^{g)}$
Si II	1260.42			$820^{g)}$	$780^{g)} + 700^{l)}$	$1040^{g)}$
O I	1302.17	$2200 \pm 150^{c)}$	$1700 \pm 150^{c)}$	$700^{g)} + 500^{l)}$	$650^{g)} + 650^{l)}$	$770^{g)}$
Si II	1304.37			$640^{g)} + 460^{l)}$	$510^{g)} + 540^{l)}$	$440^{g)}$
C II	1334.53	$1800 \pm 150^{d)}$	$1700 \pm 150^{d)}$	$970^{g)} + 740^{l)}$	$850^{g)} + 700^{l)}$	$> 1100^{o)}$
C II*	1335.70				$425^{l)}$	
Si IV	1393.76	< 100	300 ± 50	$240^{g)} + 340^{l)}$	$170^{g)} + 350^{l)}$	$150^{g)}$
Si IV	1402.82	< 100	200 ± 50	$140^{g)} + 260^{l)}$	$90^{g)} + 300^{l)}$	$120^{g)}$

: uncertain, $^{a)}$ total EW for the all three N I lines, $^{b)}$ total EW for S II λ 1259.52 and Si II λ 1260.42, $^{c)}$ total EW for O I λ 1302.17 and Si II λ 1304.37, $^{d)}$ total EW for C I λ 1334.53 and C II* λ 1335.70, $^{g)}$ galactic absorption, $^{l)}$ LMC absorption, $^{n)}$ first multiplet line only, $^{m)}$ first two multiplet lines only, $^{o)}$ galactic and LMC absorption blend.

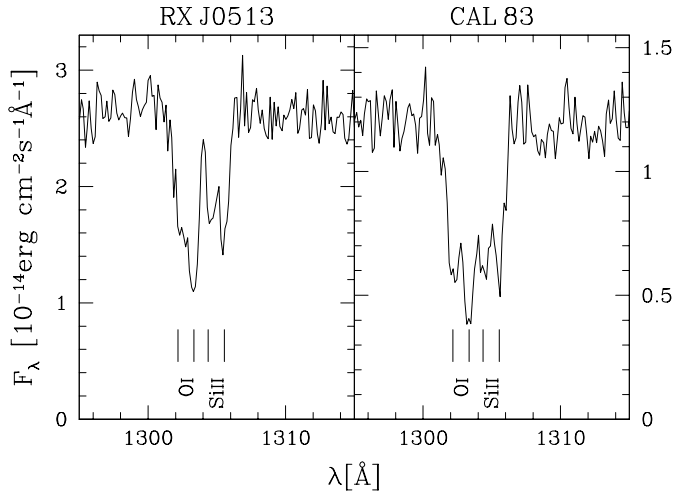

Fig. 3. Interstellar absorption lines of O I and Si II in the HST spectra of CAL 83 and RX J0513. The tick marks indicate galactic and LMC absorption set to 0 km s^{-1}and ∼+270 km s^{-1}, respectively.

interstellar equivalent widths across the LMC (excluding the central region of 30 Dor, where the absorption is higher). Table 4 shows that the galactic foreground absorption towards the three comparison stars can account for about half of the equivalent widths measured from the HST spectra of CAL 83. Including the absorption within the LMC, the total equivalent widths in the spectra of the three comparison stars are comparable in size or exceed those observed in the spectra of the two SSXBs. Even though this direct comparison may not be strictly valid as the lines of sight for the three comparison stars differ from those towards the two SSXBs, we conclude that the major part (if not all) of the absorption lines observed in CAL 83 and RX J0513 are of interstellar nature. The absorption lines from the highly ionized species as e.g. Si III, Si IV may also be partly intrinsic to the source, as observed e.g. in the ultraviolet spectra of the novalike variable IX Vel (Long et al. 1994). However, if such lines originate on the surface of the hot irradiated disc, it seems more likely that these would be in emission instead of absorption (see Sect. 3.4).

The nominal spectral resolution of the GHRS (125−150 km s^{-1}) is sufficient to resolve the galactic and LMC absorption components, being separated by $\sim$ 200 − 270 km s^{-1} (e.g. de Boer et al. 1980). This is best demonstrated on the absorption lines of O I λ 1302 and Si II λ 1304, as shown in Fig. 3. Galactic and LMC interstellar matter contribute roughly equally to the total absorption of O I λ 1302 and Si II λ 1304, as it is also observed for the three comparison stars (Table 4). Below Lyα, the low S/N prevents a clear separation of the different velocity components of Si II $\lambda\lambda$ 1191,1193 and of the N I triplet at 1200 Å. The galactic and LMC absorption can also not be resolved in C II λ 1335 as the line is strongly blended with C II* λ 1336. As mentioned in Sect. 2.1, the zero point of the wavelength calibration is uncertain by $\sim 200\,{\rm km\,s^{-1}}$. We have improved the wavelength calibration by adjusting the observed galactic absorption lines of O I λ 1302 and Si II λ 1304 to zero velocity. However, considering the complex structure of the interstellar absorption lines, an uncertainty of $\sim 100\,{\rm km\,s^{-1}}$ remains.

3.4. Emission lines

The HST spectra of CAL 83 and RX J0513 both contain N V $\lambda\lambda$ 1239,1243 emission lines. While O V λ 1371 emission is clearly observed in RX J0513, it is marginally visible in CAL 83. In RX J0513, there is also a hint for O IV λ 1345 emission. The N V doublet shows a complicated structure (Fig. 4). The two

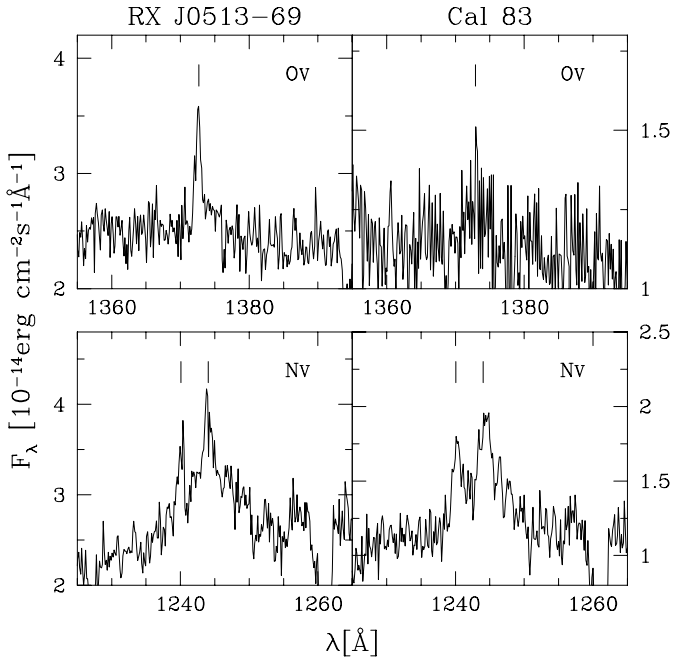

Fig. 4. Emission lines in the HST spectra of CAL 83 and RX J0513. On the red side of N v, weak absorption of S ii $\lambda\lambda$ 1250.6, 1253.8 is evident.

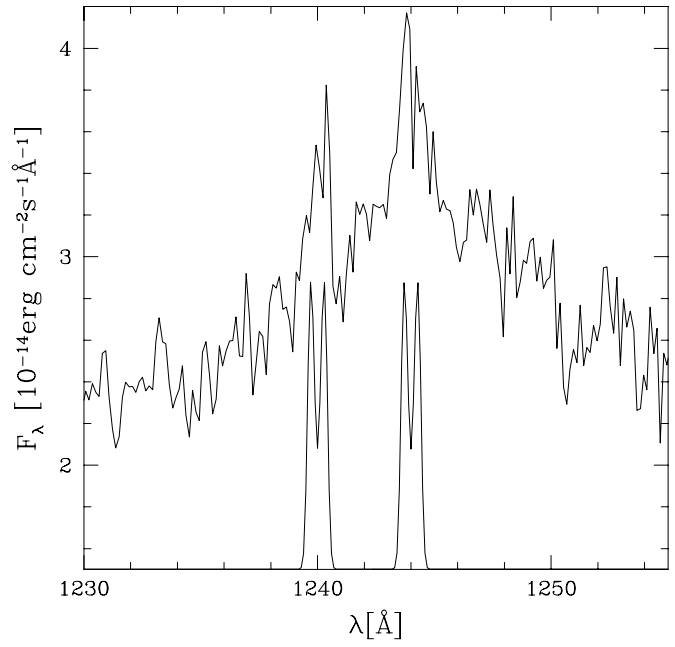

Fig. 5. The double-peaked N v emission line in RX J0513, along with the simulated Doppler-broadening of a narrow Gaussian emission in a ring rotating with $100\,\mathrm{km\,s^{-1}}$

narrow N v doublet lines have FWHM $\sim$ 1 Å and are centered (in the wavelength scale corrected as described above) at $\sim +300\,\mathrm{km\,s^{-1}}$, consistent with the measured γ velocity for the two systems (Crampton et al. 1987; Southwell et al. 1996). In RX J0513, the narrow N v lines seem to be double peaked (Fig. 5). In both systems, an additional wing extends redwards to velocities of $\sim +800\,\mathrm{km\,s^{-1}}$ relative to the system velocities. Similarly, the emission of O v in the spectrum of RX J0513 has a narrow component with FWHM ~ 0.9 Å and a tail extending to $\sim +800\,\mathrm{km\,s^{-1}}$.

The asymmetric N v and O v line profiles are reminiscent of the He ii λ 4686 emission line in the optical spectra of CAL 83, which was observed to have alternatively a blue- or redshifted wing extending up to $\sim 1000\,\mathrm{km\,s^{-1}}$(Crampton et al. 1987). Crampton et al. (1987) tentatively attribute this wing to a weakly collimated outflow with a precession period of ~ 69 d.

The wavelength range of the IUE spectra allows the study of the He ii λ 1640 line, which lies outside the wavelength range of our HST spectra. Crampton et al. (1987) detected an emission feature at 1670 Å in all their SWP spectra of CAL 83. Also the IUE spectrum of RX J0513 presented by Pakull et al. (1993) shows emission of He ii extending up to ~ 1670 Å. We have checked all SWP line-by-line spectra of CAL 83 for He ii emission extending redwards and confirm the presence of an emission feature at ~ 1666 Å without any obvious contamination by cosmic hits in four exposures of CAL 83 (SWP24554L, SWP25309L, SWP28390L and SWP33936L). In several other spectra of CAL 83 this feature seems also to be present but may be mimicked by cosmic hits. The ultraviolet bright state IUE observation of RX J0513 (SWP44467L) was performed with a second star in the slit (Pakull et al. 1993). We carefully re-extracted the spectrum of RX J0513 from the IUE image using a double Gaussian method and confirm the presence of a weak emission feature near 1666 Å. The low S/N of the IUE spectra prevents any secure identification, but we note that identifying the 1666 Å feature as Doppler shifted He ii emission would imply a velocity of $\sim 4000\,\mathrm{km\,s^{-1}}$. At optical wavelengths, RX J0513 exhibits narrow emission features close to the emission of Hα, Hβ, and He ii λ 4686. These features have been interpreted as emission from a high-velocity ($\sim 4000\,\mathrm{km\,s^{-1}}$) jet (Crampton et al. 1996, Southwell et al. 1996). Hitherto, no such jet features have been reported from optical spectroscopy for CAL 83. In contrast to the jet features observed at optical wavelengths in RX J0513, the IUE spectra of CAL 83 and RX J0513 do not show evidence for emission from the blueshifted counter jet. Considering that the redshifted jet component appears to be stronger in the optical lines of RX J0513 (Southwell et al. 1996), the limited S/N of the IUE exposures may prevent the detection of the blueshifted component of He ii λ 1640.

The origin of the narrow components of the emission lines in the HST spectra is uncertain. However, the presence of a very luminous soft X-ray source makes it unlikely that these lines are formed in low-density gas near the accreting object (see Sect. 4.1). The double-peaked structure observed in RX J0513 favours an origin from the irradiated surface of the accretion disc. As the inclination in RX J0513 is very low (e.g. Southwell et al. 1996), the projected Keplerian velocity in the disc is not sufficient to smear a sharp intrinsic emission line (for metal lines, thermal broadening dominates the intrinsic line widths). We have computed the Doppler-broadening of a rotating ring to a sharp (FWHM ~ 0.25 Å) Gaussian and find that the projected velocity of the ring must be $50\,\mathrm{km\,s^{-1}} \lesssim \mathrm{v} \lesssim 150\,\mathrm{km\,s^{-1}}$ in

order to match the observed double-peaked line profile (Fig. 5). Taking $M_{\rm wd} = 1.0\,M_\odot$ and an inclination of $i = 10°$, the criterion for v is fulfilled for $2 \times 10^{10}\,{\rm cm} \lesssim r \lesssim 2 \times 10^{11}$ cm, where r is the radius of the ring. In RX J0513, the disc is expected to have a radius of $\sim 1.5 \times 10^{11}$ cm. It appears, therefore, plausible that the observed N v emission originates from a large outer fraction of the irradiated accretion disc. In CAL 83, the accretion disc extends to larger radii and, hence, to lower velocities, possibly filling in the narrow dip in the double-peaked emission profile. However, the S/N of our GHRS spectrum of CAL 83 is a factor ~ 2 lower than that of RX J0513, which may prevent detection of a narrow double-peaked emission line profile. Nevertheless, the small width of the N v lines indicates that also the orbital inclination of CAL 83 must be low.

4. Discussion

4.1. The supersoft X-ray sources in CAL 83 and RX J0513

The determination of the luminosity and size of the supersoft X-ray sources in CAL 83 and RX J0513 has been hampered by the modest spectral resolution of the existing X-ray observations. For a large range of effective temperatures, an acceptable fit was possible by adjusting the amount of interstellar absorption. In particular for CAL 83, for which a calibration phase ROSAT PSPC spectrum with modest signal-to-noise exists, the X-ray parameters were rather uncertain. Greiner et al. (1991) derived a luminosity of $(1-10) \times 10^{38}\,{\rm ergs\,s^{-1}}$ using blackbody spectra.

With our new upper limits to the neutral hydrogen column densities towards CAL 83 and RX J0513, we can constrain the luminosities and radii of the supersoft X-ray sources in both binaries. A caveat is necessary, however, with respect to the possible presence along the line of sight of ionized matter in which hydrogen is significantly ionized, while helium and metals are not fully ionized. In consequence of this, the neutral hydrogen column density would underestimate the amount of soft X-ray absorption. This would be the case for plasmas in photoionization equilibrium with ionization parameters $\Xi \sim 1$ (Krolik & Kallman 1984), where the ionization parameter is defined as $\Xi = F/Pc$ with F the ionizing flux and P the local gas pressure. For matter close to the supersoft X-ray source, e.g. inside the Roche Lobe due to a stellar wind, $\Xi \gg 1$ unless unrealistically huge densities are involved. On the other hand, circumstellar matter, like the ionization nebula surrounding CAL 83 (Pakull & Motch 1989; Remillard et al. 1995), must have a radial range with $\Xi \sim 1$. Remillard et al. (1995) estimate that the total column density in the CAL 83 nebula is $N_{\rm H} \lesssim 10^{20}\,{\rm cm^{-2}}$, which is comparable to the uncertainty in our upper limit for the neutral hydrogen column density. The hot gas in the galactic halo also contributes to the total hydrogen column density with an amount of $\sim 50\,{\rm kpc} \times 10^{-3}\,{\rm cm^{-3}}$ which corresponds to $\sim 1.5 \times 10^{20}\,{\rm cm^{-2}}$. However, assuming a temperature of $\sim 10^6$ K, this gas does not significantly contribute to the soft X-ray absorption below ~ 0.7 keV (Krolik & Kallman 1984). We conclude that the inferred neutral hydrogen column densities towards CAL 83 and RX J0513 are a reasonable indicator for the amount of soft X-ray absorption, and we will use $N_{\rm H} < 7.5 \times 10^{20}\,{\rm cm^{-2}}$ for CAL 83 and $N_{\rm H} < 6.5 \times 10^{20}\,{\rm cm^{-2}}$ for RX J0513.

We illustrate the significance of the upper limits for the amount of soft X-ray absorption by fitting LTE high-gravity model atmosphere spectra (van Teeseling et al. 1996) to the ROSAT PSPC spectrum of CAL 83. Fig. 6 shows the 1, 2, and 3–σ confidence contours in the temperature-luminosity plane for $\log g = 8$ and $\log g = 9$. Fig. 6 shows that the upper limit for the absorption column implies two upper limits for the supersoft X-ray source in CAL 83: first, an upper limit for the bolometric luminosity of $L \lesssim 2 \times 10^{37}\,{\rm erg\,s^{-1}}$, and second, an upper limit for its radius of $R_{\rm wd} \lesssim 8 \times 10^8$ cm for $\log g = 8$ and $R_{\rm wd} \lesssim 6 \times 10^8$ cm for $\log g = 9$. We note that in both cases the best-fit absorption column is $N_{\rm H} \sim 7 \times 10^{20}\,{\rm cm^{-2}}$, consistent with no Ly$\alpha$ absorption intrinsic to the source. If we assume that $N_{\rm H} = (6.5 \pm 1.0) \times 10^{20}\,{\rm cm^{-2}}$, we obtain $R_{\rm wd} = (3-8) \times 10^8$ cm for $\log g = 8$ and $R_{\rm wd} = (2-6) \times 10^8$ cm for $\log g = 9$, both with $L = (0.7-2) \times 10^{37}{\rm ergs\,s^{-1}}$. Using the Nauenberg (1972) mass-radius relation, we find a radius of $\sim 9 \times 10^8$ cm ($\sim 4 \times 10^8$ cm) for a cold $\log g = 8$ ($\log g = 9$) white dwarf. Because at most half of the white dwarf can be obscured from view by the accretion disk, these results suggest that the shell-burning white dwarf in CAL 83 has not expanded by more than a of factor ~ 2 (e.g. a $1.2 M_\odot$ white dwarf with a radius of $\sim 10^9$ cm) compared to the Nauenberg radius. However, the results are consistent with a white dwarf which has not expanded at all.

From the Hα and [O III] λ 5007 emission of the nebula surrounding CAL 83, Remillard et al. (1995) infer a *time-averaged* ionizing luminosity of $\sim (1-4) \times 10^{37}\,{\rm erg\,s^{-1}}$, which is consistent with the luminosity from our spectral fits. This indicates that there is no need to assume that during a significant fraction of the past $\sim 10^4$ years the hydrogen shell burning has been turned off, as has been suggested by Remillard et al. (1995).

The low luminosity of CAL 83 is surprising in the context of the steady-burning model for SSXBs. Using a luminosity $\lesssim 2 \times 10^{37}{\rm ergs\,s^{-1}}$, the stability line in Fig. 1 of Iben (1982) indicates that the white dwarf in CAL 83 is either not burning the accreted matter in a steady state, i.e. the hydrogen is not burned at precisely the accretion rate, or the white dwarf is not very massive ($M_{\rm wd} \lesssim 0.8\,M_\odot$). Such a low mass, however, seems to be inconsistent with the high observed temperature and the rapid decline during the X-ray off state (Alcock et al. 1997).

For RX J0513, the upper limit on the column density $N_{\rm H}$ confirms the parameters determined with χ^2 fits of model atmosphere spectra to the ROSAT PSPC spectrum of July 1993. These fits give $N_{\rm H} = (4-7) \times 10^{20}\,{\rm cm^{-2}}$, $L = (2.5-9) \times 10^{37}\,{\rm erg\,s^{-1}}$, and, for $\log g = 8$, $R_{\rm wd} = (6-12) \times 10^8$ cm ($R_{\rm wd} = (4-9) \times 10^8$ cm for $\log g = 9$).

4.2. Long-term variability

Even though CAL 83 and RX J0513 are virtually spectroscopic twins, the long-term variability observed in both sources suggests a systematic difference of the accretion rate in the two systems.

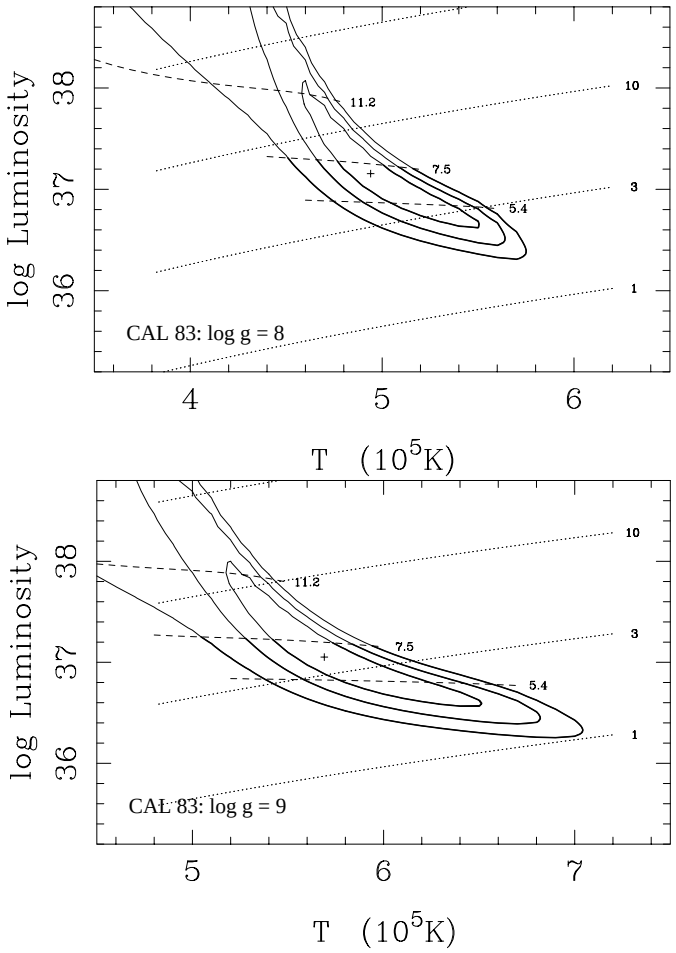

Fig. 6. χ^2 contours at 1, 2, and 3–σ confidence levels for fits of $\log g = 8$ (upper panel) and $\log g = 9$ (lower panel) LTE model atmospheres to the ROSAT X-ray spectrum of CAL 83. The dashed lines connect points of equal absorption column density in units of $N_{\rm H} = 10^{20}$ cm^{-2}; the dotted lines connect points of equal white dwarf radius in units of 10^8 cm. The part of the contours below the upper limit of $N_{\rm H} < 7.5 \times 10^{20}$ cm^{-2} inferred from the Lyα profile is shown thicker

RX J0513 shows quasi-regular (every ~ 150 days) optical low states ($\Delta V \approx 1$ mag), which are accompanied with a turn-on of X-ray emission. This inverse variability at optical and X-ray wavelengths has been successfully modeled by expansion/contraction of the white dwarf photosphere, as described in the Introduction and e.g. by Reinsch et al. (1996). In this model, the bolometric luminosity of the white dwarf remains roughly constant if the white dwarf radius changes. However, during the expansion phase, the irradiating spectrum becomes softer (but the bulk is still emitted at energies above the Lyman edge). The fact that RX J0513 and CAL 83 have very similar ultraviolet spectra, while RX J0513 was probably observed during an X-ray off state and CAL 83 during an X-ray on state (the normal state for both sources, see Sect. 3.1), suggests that in both sources the accretion-disc flux was dominated by irradiation from the accreting white dwarf. This argues against a significant *bolometric* fading of the shell-burning white dwarf during the X-ray off state of RX J0513 and is consistent with the expansion/contraction model (Reinsch et al. 1996). A possible cause for the contraction of the white dwarf photosphere could be a slightly decreased accretion rate. Southwell et al. (1996) suggest that star spots on the secondary cover the L_1 point, resulting in a decreased mass loss rate from the secondary, a model originally suggested by Livio & Pringle (1994) for the VY Scl stars.

CAL 83 is an almost persistent bright X-ray source. The only X-ray turn-off observed so far (Kahabka 1997) was accompanied with an optical *dip* and has been explained by a decrease of the accretion rate with subsequent extinction of the nuclear burning on the white dwarf surface (Alcock et al. 1997). The long-term light curve of CAL 83 compiled from the IUE archive shows a rare ultraviolet bright state ($\Delta_{\rm UV} \approx 1$ mag). A plausible, but speculative hypothesis is that, similarly to the *normal* state of RX J0513, the observed ultraviolet bright state in CAL 83 was due to an expansion of the white dwarf photosphere. This hypothesis could be confirmed if another ultraviolet/optical brightening will be accompanied by an X-ray turn-off. A brightening due to expansion of the white dwarf cannot be explained with the star-spot model, as this would require a sudden *increase* of the accretion rate. However, in the case of stable, but non-steady-state H-burning, as suggested by the low luminosity of CAL 83 (Sect. 4.1), the ultraviolet/optical brightening may also be caused by an episode of increased nuclear energy release at *constant* accretion rate. Whether in this case the ultraviolet/optical brightening will be accompanied also by an X-ray brightening depends on the response of the white dwarf radius.

5. Conclusion

Our HST/GHRS observations of the two SSXBs CAL 83 and RX J0513 show that the two sources have very similar ultraviolet spectra: almost flat continua are overlayed by strong interstellar absorption lines of both galactic and LMC origin. The intrinsic spectra of the two SSXBs appear to be featureless except for emission lines of N v and O v with narrow components at the system velocity and red wings extending to $\sim +800\,{\rm km\,s^{-1}}$. Evidence for high-velocity components of He ii is found in the IUE spectra. A likely origin of the narrow components is the irradiated surface of the outer accretion disc, indicating a low inclination for both systems.

The broad interstellar Lyα absorption profile yields neutral hydrogen column densities of $N_{\rm HI} = (6.5 \pm 1.0) \times 10^{20}{\rm cm}^{-2}$ for CAL 83 and $N_{\rm HI} = (5.5 \pm 1.0) \times 10^{20}{\rm cm}^{-2}$ for RX J0513, very similar to the galactic foreground column density, indicating that LMC or intrinsic absorption contribute little to the total column density. These independent estimates of $N_{\rm HI}$ constrain the X-ray luminosity of CAL 83 to be $(0.7-2) \times 10^{37}\,{\rm ergs\,s^{-1}}$, which is at the lower end of the stable burning strip. For RX J0513, we find $(2.5-9) \times 10^{37}\,{\rm ergs\,s^{-1}}$.

The long-term ultraviolet light curve of CAL 83 displays a rare brightening, possibly due to an episodic expansion of the white dwarf photosphere. Further long-term monitoring of this source, both at optical and X-ray wavelengths is needed to clarify the nature of this bright state.

Acknowledgements. We thank Howard Lanning for the support in preparing the HST observations and the referee K.S. de Boer for constructive criticism. This work was supported in part by the DARA under project number 50 OR 9210.

References

Alcock C., Allsman R.A., Alves D., et al., 1997, MNRAS 286, 483
Bessell M.S., 1991, A&A 242, L17
Bianchi L., Pakull M.W., 1988, in *A Decade of UV Astronomy with IUE*, Rolfe E.J. (ed.), ESA-SP 281, 145
Blades J.C., Wheatley J.M., Panagia N., et al., 1988, ApJ 334, 308
de Boer K.S., Savage B.D., 1980, ApJ 238, 86
de Boer K.S., Koornneef J., Savage B.D., 1980, ApJ 236, 769
Bohlin R.C., 1975, ApJ 200, 402
Bohlin R.C., Savage B.D., Drake J.F., 1978, ApJ 224, 132
Crampton D., Cowley A.P., Hutchings J.B., et al., 1987, ApJ 321, 745
Crampton D., Hutchings J.B., Cowley A.P., et al., 1996, ApJ 456, 320
Dickey J.M., Lockman F.J., 1990, ARA&A 28, 215
Fitzpatrick E.L., 1986, AJ 92, 1068
Gänsicke B.T., Beuermann K., de Martino D., 1996, in Supersoft X-ray Sources, Greiner J. (ed.), Lecture Notes in Physics 472, p. 105
Greiner J. (ed.), 1996, *Supersoft X-ray sources*, Lecture Notes in Physics 472 (Berlin: Springer)
Greiner J., Hasinger G., Kahabka P., 1991, A&A 246, L17
Hutchings J.B., Cowley A.P., Schmidtke P.C., Crampton D., 1995, AJ 110, 2394
Iben I., 1982, ApJ 259, 244
Kahabka P., 1997, IAU Circ. No. 6432
Krolik H.K., Kallman T.R., 1984, ApJ 286, 366
Leitherer C., Koratkar A., Lupie O., Hulber S. 1994, GHRS Instrument Science Report 68
Livio M., Pringle J.E., 1994, ApJ 427, 956
Long K.S., Wade R.A., Blair W.P., Davidson A.F., Hubeny I., 1994, ApJ 426, 704
Nauenberg M., 1972, ApJ 175, 417
Pakull M.W., Motch C., 1989, in *Extranuclear Activity in Galaxies*, Meurs E.J.A., Fosbury R.A.E. (eds.), Garching: ESO, p. 285
Pakull M.W., Motch C., Bianchi L., et al., 1993, A&A 278, L39
Remillard, R.A., Rappaport S., Macri L.M., 1995, ApJ 439, 646
Reinsch K., van Teeseling A., Beuermann K., Abott T.M.C., 1996, A&A 309, L11
Rohlfs K., Kreitschmann J., Siegman B.C., Feitzinger J.V., 1984, A&A 137, 343
Savage B.D., de Boer K.S., 1979, ApJ 230, L77
Savage B.D., de Boer K.S., 1981, ApJ 243, 460
Schaeidt S., 1996, in *Supersoft X-ray sources*, Greiner J. (ed.), Lecture Notes in Physics 472, p. 159 (Berlin: Springer)
Schaeidt S., Hasinger G., Trümper J., 1993, A&A 270, L9
Sion E.M., Starrfield S.G., 1994, ApJ 421, 261
Southwell K.A., Livio M., Charles P.A., O'Donoghue D., Sutherland W.J., 1996, ApJ 1065
van den Heuvel E.P.J., Bhattacharya D., Nomoto K., Rappaport S.A., 1992, A&A 262, 97
van Teeseling A., Heise J., Kahabka P., 1996, in *Compact Stars in Binaries*, IAU Symp. 165, van Paradijs J., et al. (eds.), Kluwer Academic Publishers
Zimmermann H.U., Becker W., Belloni T., et al., 1994, MPE Report 257